Inference techniques for the analysis of Brownian image textures.

Frédéric RICHARD

Institut de Mathématiques de Marseille, Aix-Marseille Université.

Journées Statistiques du Sud 2024
june, 19-21, 2024.

Context and goal

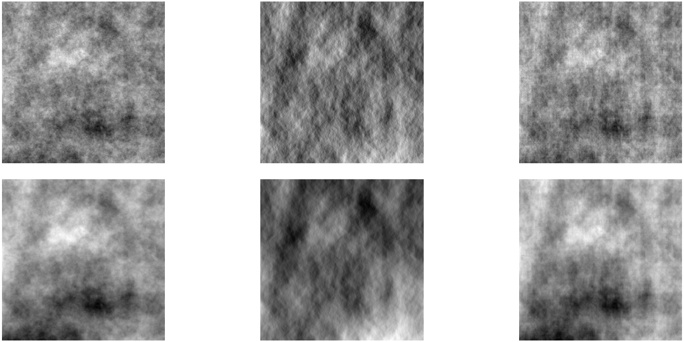

- Context: analysis of rough anisotropic textures of images,
- Goal: statistical analysis of these textures, classification.

Related topic: analysis of texture heterogeneity

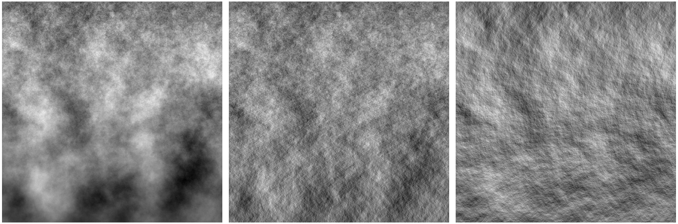

- Context: analysis of textures of irregular images.
- Aim: characterization of heterogeneity in terms of
  - regularity,
  - directional properties (anisotropy).

Stationary fields

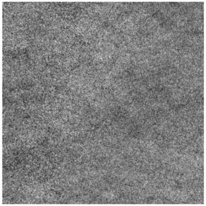

Details of a photographic film (Messier coll.)

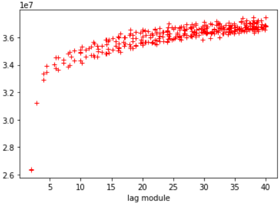

Its empirical semi-variogram.

- Random field : $\{Z(x), x \in \mathbb{R}^d\}$,
- (Second-order) stationarity : spatial invariance of
  - mean : $\mathbb{E}(Z(x)) = m, \forall\, x$ ($\Rightarrow$ no trend),
  - covariance : $c(h) = \mathrm{Cov}(Z(x+h), Z(x)), \forall\, h$.
- Semi-variogram :
  - $v(h) = \frac{1}{2}\mathrm{E}((Z(x+h) - Z(x))^2)$.
  - $\lim_{|h| \to +\infty} v(h) = v_0 < +\infty$.

Non stationarity

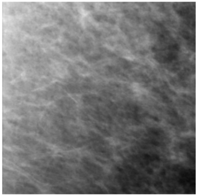

Detail of a mammogram

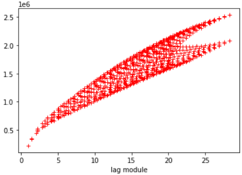

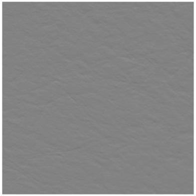

Vertical increments

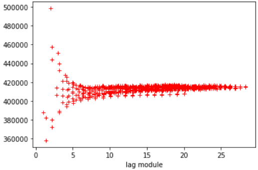

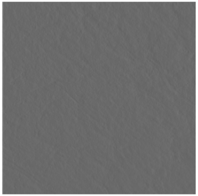

Horizontal increments

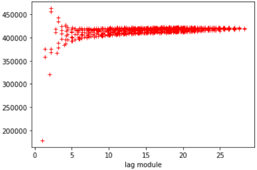

Fields with stationary increments

- Given two positions $x_1, x_2 \in \mathbb{R}^2$, $V_x = Z(x_1) - Z(x_2)$ is a field increment, and

$$\left\{ V_x(y) = Z(x_1 + y) - Z(x_2 + y), y \in \mathbb{R}^2 \right\}$$

an increment field.

- A field Z has stationary increments if, for any couple of positions $x = (x_1, x_2)$, the increment field $V_x(\cdot)$ is stationary, i.e. for any y and z
  - $\mathbb{E}(V_x(y)) = a$,
  - $\mathbb{E}(V_x(y)V_x(z)) = K_x(y - z)$.
- If Z is square integrable with stationary increments, then
  - $\mathbb{E}(Z(x)) = \langle x, a \rangle + m$,
  - the semi-variogram is unbounded.

Trends

Photographic film (Messier collection)

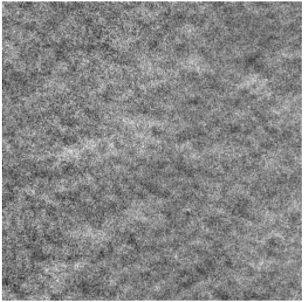

Crop of the processed image.

Intrinsic random fields

- An increment $V_x = Z(x_1) - Z(x_2)$ annihilates constants.
- *M*-increment : $Z_{\lambda,x} = \sum_{i=1}^{m} \lambda_i Z(x_i)$

$$\sum_{i=1}^{m} \lambda_i P(x_i) = 0, \forall P, \text{polynomial } \ d^o P \leq M$$

M-IRF: fields with zero-mean stationary *M*-increment fields, *i.e.* fields $V_{\lambda,x}(y) = \sum_{i=1}^{m} \lambda_i Z(x_i + y)$ satisfy

$$\mathbb{E}(V_{\lambda,x}(y)) = 0, \forall\, y \in \mathbb{R}^d,$$
$$\mathbb{E}(V_{\lambda,x}(y) V_{\lambda,x}(z)) = K_{\lambda,x}(y - z), \forall\, y, z \in \mathbb{R}^d.$$

- A *M*-IRF may have a polynomial trend of order *M*.

Correlation structure of an IRF

- **Stationary fields** are characterized by a covariance C, which is definite positive, i.e.

$$\mathbb{E}(Z_{\lambda,x} Z_{\mu,y}) = \sum_{i=1}^{m} \sum_{j=1}^{n} \lambda_i \, \mu_j C(x_i - y_j) \geq 0, \qquad (1)$$

  for any linear combinations $Z_{\lambda,x}$ and $Z_{\mu,y}$.

- Continuous *M*-**IRFs** Z are characterized by generalized covariances C that are *M*-conditionally positive-definite, i.e. Eq. (1) holds for any M-increments $Z_{\lambda,x}$ and $Z_{\mu,y}$.

Spectral representations (with a density)

- Spectral representation of stationary field covariance:

$$c(h) = \int_{\mathbb{R}^2} \cos(\langle h, w \rangle) f(w) dw,$$

with $\int_{\mathbb{R}^2} f(w)dw < \infty$ (Bochner theorem).

- Spectral representation of generalized covariances [Ref. Gelfand & Villenkin, 1964; Matheron 1973].

$$C(h) = \int_{\mathbb{R}^2} \left(\cos(\langle w, h \rangle) - \mathbf{1}_{B(0,\epsilon)}(w) P_M(\langle w, h \rangle) \right) f(w) dw,$$

with $P_M(t) = 1 - \frac{t^2}{2} + \cdots + \frac{(-1)^M}{(2M)!} t^{2M}$, and $\forall \epsilon > 0$,

$$\int_{|w|<\epsilon} |w|^{2M+2} f(w) dw < \infty, \text{ and } \int_{|w|>\epsilon} f(w) dw < \infty.$$

The M-anisotropic fractional Brownian field

- Zero mean M-IRF with a spectral density of the form

$$f(w) = \tau\left(\frac{w}{|w|}\right)|w|^{-2\beta\left(\frac{w}{|w|}\right)-d}.$$

- determined by two directional functions:
  - the topothesy function τ: $\tau(s) \geq 0$
  - the Hurst function β: $\beta(s) > 0$ and

$$H = \min\{\beta(s), s \in S, \tau(s) > 0\} \in (0, 1),$$

- Polynomial trend of order $M =$.
- Extension of 0-intrinsic field defined by [Bonami and Estrade, 2004].

[Ref. Richard, 2016].

A model for image micro-textures.

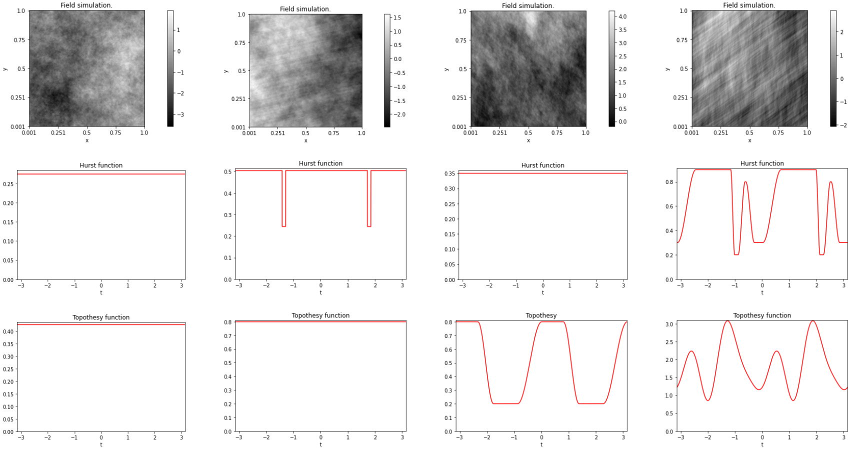

Field irregularity.

- $H \in (0, 1)$: critical Hölder exponent of a field Z if, on a compact set C and for a positive random variable A

$$|Z(x) - Z(y)| \leq A|x - y|^{\alpha}$$

holds with probability one for any $\alpha < H$, but not for $\alpha > H$.

- Spectral characterization for IRF
[Ref. Bonami and Estrade, 2004; Biermé, 2005].
(i) If $\forall 0 < \alpha < H$, $\exists A_1, B_1 > 0$,

$$|w| \geq A_1 \Rightarrow f(w) \leq B_1 |w|^{-2\alpha - d},$$

then the field Z is Hölder of order $\geq H$.
(ii) If $\forall H < \beta < 1$, $\exists A_2, B_2 > 0$, a pos. meas. subset E s.t.

$$|w| \geq A_2 \text{ and } \arg(w) \in E \Rightarrow f(w) \geq B_2 |w|^{-2\beta - d},$$

then the field Z is Hölder of order $\leq H$.

Asymptotic topothesy

Irregularity determined by the order H of Hölder irregularity.

Directional properties characterized by the asymptotic topothesy:

$$\tau^*(s) = \lim_{\rho \to +\infty} f(\rho s)\rho^{2H+d}.$$

- $E_0 = \{s, \tau^*(s) > 0\}$ gathers directions where
  - density convergence is at lowest speeds of order ρ^{2H+d},
  - high-frequencies are the largest.
- Proposition (ii): due to high-frequencies in these directions, the field irregularity is as low as H.
- The larger $\tau^*(s)$, the larger high-frequencies in s.
- The asymptotic topothesy τ^* quantifies contributions of directional high-frequencies to the field irregularity.

An example of texture classification.

Microscopic images of photographic films (source: Paul Messier, MoMA, NY).

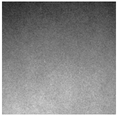

Glossy

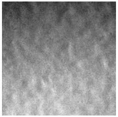

Semi-glossy

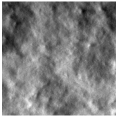

Matte

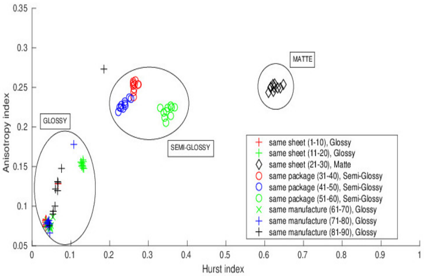

Hurst index : $H = \arg\min_s \{\beta(s), \tau(s) > 0\}$.

Asymptotic topothesy: $\tau^*(s) = \tau(s)$ if $\beta(s) = H$ and 0 otherwise.

Anisotropy index: $I = \frac{\sqrt{\int (\tau^*(s) - \overline{\tau^*})^2 ds}}{\overline{\tau^*}}$, with $\overline{\tau^*} = \int \tau^*(s) ds$.

[FR, Stat & Comput, 2018; Spatial Stat, 2017].

Heterogeneous models

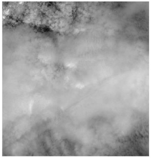

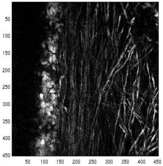

Satellite image (Sentinel, CNES)   Biphoton microscopy (La Timone, AMU)

Multifractional Brownian fields [Benassi et al, 1997]:

$$Z(x) = C_x \int_{\mathbb{R}^d} \frac{e^{i\langle x,\omega\rangle} - 1}{|\omega|^{H_x + d/2}} \, d\widehat{W}(\omega)$$

Anisotropic multifract. Brownian fields [Polisano, 17; FR and Vu, 18]:

$$Z(x) = \int_{|w|>A} (e^{i\langle x,\omega\rangle} - 1)\sqrt{h_{\tau_x,\beta_x}(\omega)} \, d\widehat{W}(\omega),$$

where $h_{\tau_x,\beta_x}(\omega) = \tau_x(\omega)|\omega|^{2\beta_x(\omega)-d}$ (with assumptions on τ and β)

Tangent fields

Theorem (Polisano, 2017; FR & Vu, 2018)

Let $x \in \mathbb{R}^d$ *and* $H_x = \operatorname*{ess\,inf}_{s \in \mathcal{S}} \ \beta_x(s)$. *Then,*

$$\lim_{t \to 0^+} \left(\frac{Z(x+tu) - Z(x)}{t^{H_x}} \right)_{u \in \mathbb{R}^d} = (\tilde{Z}_x(u))_{u \in \mathbb{R}^d},$$

for a tangent field

$$\tilde{Z}_x(y) = \int_{\mathbb{R}^d} (e^{i\langle y, \omega \rangle} - 1) \sqrt{h_{\tau_x^*, H_x}(\omega)} \, dW(\omega),$$

determined by a density $h_{\tau_x^*, H_x}(\omega) = \tau_x^*(\omega) |\omega|^{2H_x - d}$ *defined with a local asymptotic topothesy*

$$\tau_x^*(w) = \begin{cases} \tau_x(w) & \text{if } \beta_x(w) = H_x, \\ 0 & \text{otherwise.} \end{cases}$$

Examples of texture segmentations

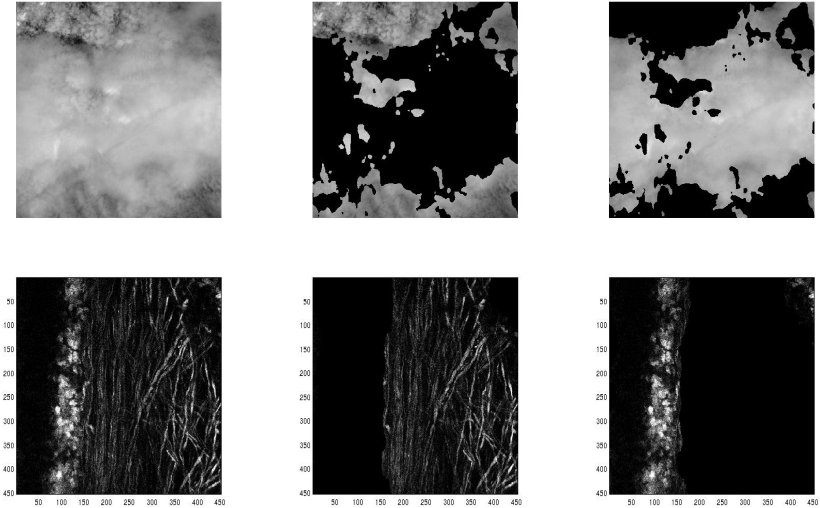

Fré

e

[FR, Stat sinica, 2015]

Inference setting

- $Y = (Y[i])_i$: image at some grid points $i \in [\![1, l]\!]^2$,
- Z: 0-AFBF with unknown semi-variogram $v(\cdot; \tau, \beta)$,
- $W = (W[i])_i$ centered Gaussian noise of variance τ_0.
- Observation model:

$$Y[i] = Z\left(\frac{i}{l}\right) + W[i], i \in [\![1, l]\!]^2.$$

- Goal: estimate τ and β from Y.

Turning-band approximation

- Semi-variogram of an AFBF (in polar coordinates):

$$v_0(h;\tau,\beta) = \frac{1}{2}\int_{-\pi/2}^{\pi/2} \nu_{\beta(\theta)}\tau(\theta)\,|\langle h, u(\theta)\rangle|^{2\beta(\theta)}\,d\theta,$$

with $u(\theta) = (\cos\theta, \sin\theta)$ and a constant ν_H.

- Can be approximated by a semi-variogram of the form

$$v(x;\tau,\beta) = \frac{1}{2}\sum_{m=1}^{M} \tilde{\tau}(\theta_m)|\langle x, u(\theta_m)\rangle|^{2\beta(\theta_m)},$$

for some appropriate angles θ_m in $[-\frac{\pi}{2}, \frac{\pi}{2}]$.

- Corresponds to the semi-variogram of a turning-band field

$$Z_M(x) = \sum_{m=1}^{M} \sqrt{\tilde{\tau}(\theta_m)}Y_m(\langle x, u(\theta_m)\rangle),$$

Y_m being a fractional Brownian motion of Hurst index $\beta(\theta_m)$.

[H. Biermé, L. Moisan, FR, J Comput Graphic Stat, 2015].

The inverse problem

- The semi-variogram of the observation $Y = Z() + W$ is approached by

$$w(x;\tau,\beta) = \tau_0 + v(x;\tau,\beta)$$

- It is fitted to the empirical semi-variogram of Y at some lags $(x_n)_n$:

$$\widehat{w}_n = \frac{1}{N_n}\sum_i (Y[i+x_n] - Y[i])^2,$$

- by minimizing the least-square criterion

$$h(\tau,\beta) = \frac{1}{2}\sum_{n=1}^{N}\left(w(x_n;\tau,\beta) - \widehat{w}_n\right)^2.$$

A non-linear separable least square criterion

- With function representations,

$$\tau(\theta) = \sum_{j=1}^{J} \tau_j T_j(\theta) \quad \text{and} \quad \beta(\theta) = \sum_{k=1}^{K} \beta_k B_k(\theta).$$

- express h as a non-linear separable least square criterion

$$h(\tau, \beta) = \frac{1}{2} \sum_{n=1}^{N} (F_n(\beta)\tau - \widehat{w}_n)^2,$$

F_n being a vector-valued function with components $F_n(\beta)_{nj} = w(x_n; T_j, \beta)$ for $j \neq 0$ and $F(\beta)_{n0} = 1$.

[Escande and FR, TPMS, 2024]

A variable projection method.

VARPRO [Golub and Peyrera, 2003]:

- Define
$$g(\beta) = h(\tau^*(\beta), \beta),$$
where, for a fixed β, $\tau^*(\beta) \in \arg\min_\tau h(\tau, \beta)$.
- Minimize g instead of h (with a Gauss-Newton method).

Our implementation:

- Multi-grid approach: successive minimization in embedded finite dimensional subspaces of piecewise constant functions.
- Definition of a "non-redundant" set of lags (x_n) to avoid problem to be ill-posed.
- Levenberg-Marquardt to find minimizers of h w.r.t. τ and g.
lsq_linear, **least_square** of package *Optimize* of Python library *Scipy*.
- Constraints to ensure that $\beta \in (0, 1)$ and $\tau \geq 0$.

Numerical study.

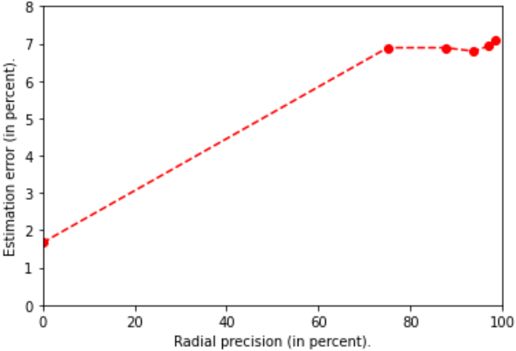

- Radial precision: $(1 - 1/M)\%$ where M is the number of intervals for the approximation β by piecewise constant funtions.
- Error: L1 error between the estimated and true values of β.
- Number of experiments: 100.
- Image size: 1024×1024.

Estimating texture models from mammograms.

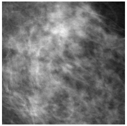
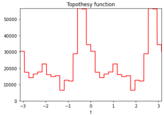

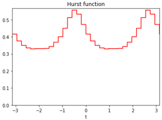

$H = 0.33$, $H_l = 0.23$, $\beta_{std} = 0.08$, $\beta_{tv} = 0.03$, $\tau_{std} = 0.63$, $\tau_{tv} = 0.32$.

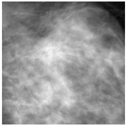
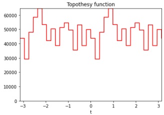

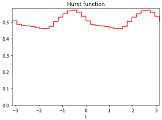

$H = 0.46$, $H_l = 0.11$, $\beta_{std} = 0.04$, $\beta_{tv} = 0.01$, $\tau_{std} = 0.19$, $\tau_{tv} = 0.23$.

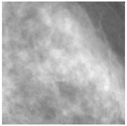
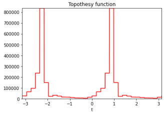

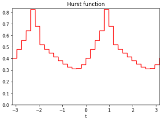

$H = 0.31$, $H_l = 0.51$, $\beta_{std} = 0.14$, $\beta_{tv} = 0.06$, $\tau_{std} = 2.07$, $\tau_{tv} = 1.09$.

Sampling realistic textures.

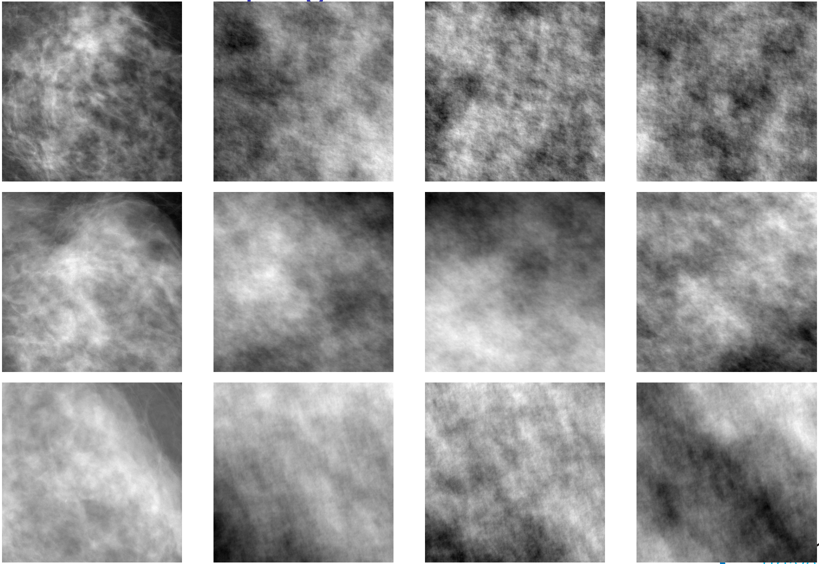

original synthetic 1 synthetic 2 synthetic 3.

Analysis of the mammogram regularity.

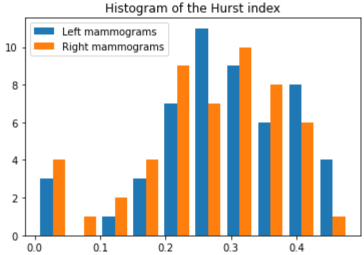

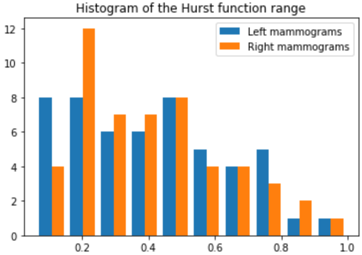

Analysis of full-field digital mammograms of 58 patients (courtesy of Dpt of Radiology, University of Pennsylvania).

Analysis of the mammogram anisotropy.

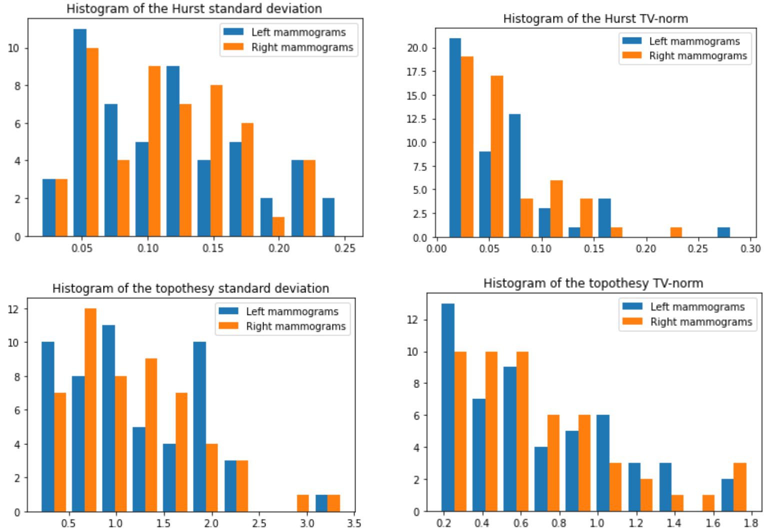

Semi-variogram shape of stationary fields.

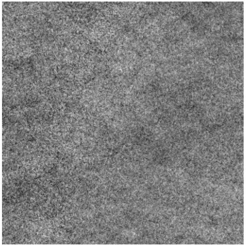

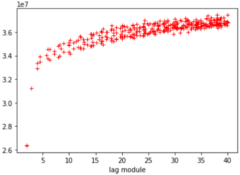

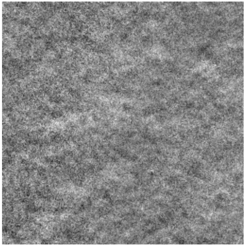

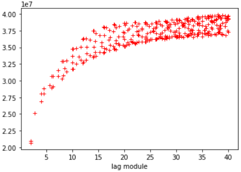

Photographic films from the collection of Paul Messier (MOMA)

Stationary turning-band fields.

- Consider a semi-variogram of the form

$$v_\kappa(x;\tau,\beta) = \frac{1}{2}\sum_{m=1}^{M} \tilde{\tau}(\theta_m) w_\kappa(\langle x, u(\theta_m)\rangle).$$

where

$$w_\kappa(t) = 2|\kappa|^{2\beta(\theta_m)} + 2|t|^{2\beta(\theta_m)} - |\kappa - t|^{2\beta(\theta_m)} - |\kappa + t|^{2\beta(\theta_m)}.$$

- Corresponds to the semi-variogram of a turning-band field

$$Z_M(x) = \sum_{m=1}^{M} \sqrt{\tilde{\tau}(\theta_m)} Y_m(\langle x, u(\theta_m)\rangle),$$

Y_m being an increment of step κ of a fractional Brownian motion of Hurst index $\beta(\theta_m)$.

Fitting semi-variograms of stationary fields.

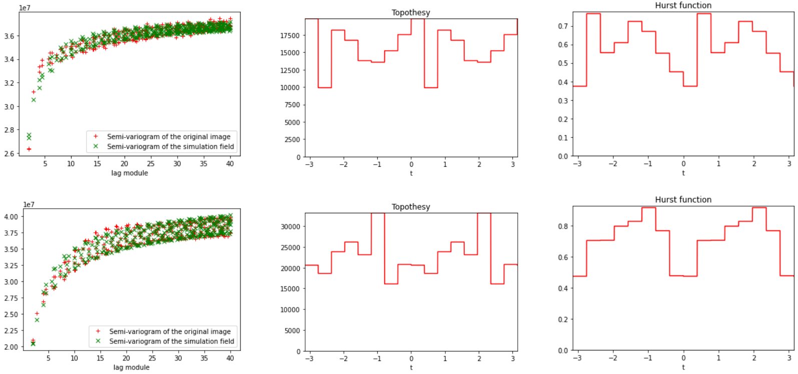

Simulation of stationary fields.

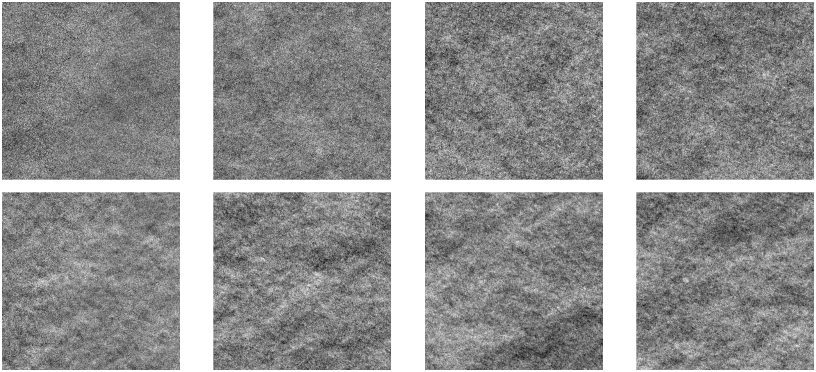

original | synthetic 1 | synthetic 2 | synthetic 3

Limitations.

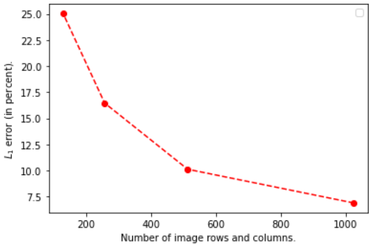

(a) effect of image size

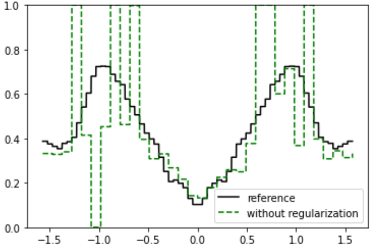

(b) numerical instabilities

- (a): 100 experiments with a radial precision of 87.5 % (8 parameters).
- L1 error without estimation of the semi-variogram (¡2%).

Penalized criterion

Minimize a penalized least square criterion

$$h(\tau, \beta) = \frac{1}{2} \sum_{n=1}^{N} (F_n(\beta)\tau - \widehat{w}_n)^2 + \alpha |D\tau|_2^2,$$

where D is a finite difference operator of order 2.

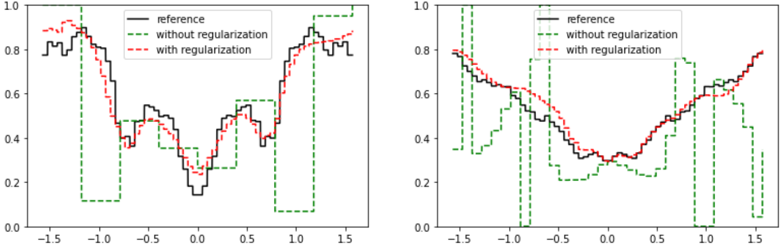

Instability monitoring.

Numerical study.

- Radial precision: 98 % (64 parameters).
- Image size 512 $\times$ 512.
- 100 experiments.

	without regularization	with regularization
Bias	0	0
RMSE	21.5	8.1
L1-error	16.22	6.4

Work in progress: Minimize a penalized least square criterion

$$h(\tau, \beta) = \frac{1}{2} \sum_{n=1}^{N} (F_n(\beta)\tau - \widehat{w}_n)^2 + \alpha |D\tau|_2^2 + \gamma |D\beta|_1^2.$$

Adaptation of the variable projection method.

Conclusion (Part 1).

- A model for image microtextures:
  - can be simulated,
  - can be fully estimated,
  - can serve for texture classification.
- Remaining challenge:
  - local estimation of the model,
  - use the model for image segmentation.

Local regularity of textures

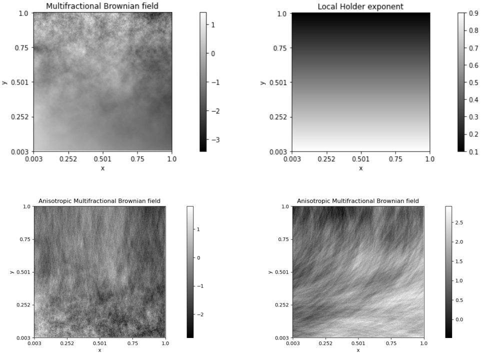

Local Hölder exponent H_x of a field Z at position x

$$H_x \underset{\text{a.s.}}{=} \sup \left\{ \alpha, \exists \rho > 0, \sup_{y \neq y' \in B(x,\rho)} \frac{|Z(y) - Z(y')|}{|y - y'|^{\alpha}} < +\infty \right\}$$

Multifractional anisotropic fractional Brownian field

Gaussian field defined by

$$\tilde{Y}_{\tau,\beta}(x) = \int_{\mathbb{R}^2} \left(e^{i\langle \omega, x\rangle} - 1\right) \sqrt{\tau_x(\arg \omega)} \|\omega\|^{-\beta_x(\arg\omega)-1} d\widehat{W}(\omega),$$

where W is a complex Brownian measure and, τ_x and β_x, two spatially varying functions (topothesy and Hurst functions).

Let

$$H_x = \operatorname{ess\,inf}_s \{\beta_x(s), \tau_x(s) > 0\},$$

and

$$\tilde{\tau}_x(s) = \tau_x(s) \mathbf{1}_{\beta_x(s) = H_x}.$$

Then, $\tilde{Y}_{\tau,\beta}$ is tangent at x (l.a.s.s.) to an AFBF of topothesy and Hurst functions $\tilde{\tau}_x$ and H_x.

Hölder regularity at x given by H_x.

[ref. Benassi et al, 97; Polisano et al, 2014; Vu and R., 2020]

Estimation of the local regularity.

Previous works:

- Quadratic variations: Coeurjoly, 2001; Vu et R., 2020.
- Wavelet leaders coupled with a regularization by total variation: Pascal, Pustelnik, Abry, 2021.

Main numerical challenges:

- achieve a good spatial precision,
- be robust to image noise and transforms (e.g. encoding of image values),
- develop benchmarks.

Local analysis of images.

- Let Z be observed on a grid: $Z^N[m] = Z(\frac{m}{N}), m \in [\![1, N]\!]^2$.
- Given some $u_{jk} = \rho_{jk}(\cos\varphi_j, \sin\varphi_j) \in \mathbb{Z}^2 \backslash \{(0,0)\}$, rescale the image of a factor ρ_{jk} and rotate it of an angle φ_k

$$T_{jk} = \rho_{jk} \begin{pmatrix} \cos(\varphi_j) & -\sin(\varphi_j) \\ \sin(\varphi_j) & \cos(\varphi_j) \end{pmatrix}.$$

- Convolve the transformed images

$$V_{jk}^N[m] = \sum_n v[n] Z^N[m - T_{jk} n]$$

  with a kernel v annihilating polynomials of order < 2.
- Compute the quadratic variations in neighborhood of some positions x_i:

$$W_{ijk}^N = \frac{1}{|\mathcal{V}_N|} \sum_{m \in \mathcal{V}_N} (V_{jk}^N[m + p_i])^2.$$

Estimation of the local Hurst index

Theorem (Ref. Hu and F.R., 2020)

Let $Y_{ijk}^N = \log(W_{ijk}^N)$ and $x_{jk0} = \log(\rho_{jk}^2)$. Then, under appropriate assumptions,

$$N^{\frac{d}{2}}(Y^N - \zeta^N) \xrightarrow[N\to+\infty]{d} \mathcal{N}(0,\Sigma),$$

for a covariance matrix Σ, and an expectation ζ^N of the form

$$\zeta_{ijk}^N = x_{jk0} H_{x_i} + \beta_{ij}^N.$$

Estimation: For any i, let $\theta_{(i)} = (H_{x_i}, \beta_{i1}^N, \cdots, \beta_{iJ}^N)^T$, then

$$\zeta_{(i)}^N = X\theta_{(i)} + \epsilon, \text{with } \epsilon \sim \mathcal{N}(0, \Sigma_{(i)})$$

So that

$$\widehat{H}_{x_i} = (1, 0, \cdots, 0)(X^T \Sigma_{(i)}^{-1} X)^{-1} X^T \Sigma_{(i)}^{-1} Y_i^N$$

Analogy with neural networks

- Construction of a feature vector:
  - Convolution layer:

$$V_{jk}^N[m] = \sum_n v[n] Z^N[m - T_{jk} n] = \sum_n v_{jk}[k] Z^N[m - n].$$

  - Square activation: $(V_{jk}^N[m])^2$
  - Average pooling:

$$W_{ijk}^N = \frac{1}{|\mathcal{V}_N|} \sum_{m \in \mathcal{V}_N} (V_{jk}^N[m + p_i])^2.$$

  - Log activation:

$$Y_{ijk}^N = \log(W_{ijk}^N)$$

- Regression with a dense layer:

$$\widehat{H}_{x_i} = (1, 0, \cdots, 0)(X^T \Sigma_{(i)}^{-1} X)^{-1} X^T \Sigma_{(i)}^{-1} Y_i^N.$$

Design of the CNN: convolutional part

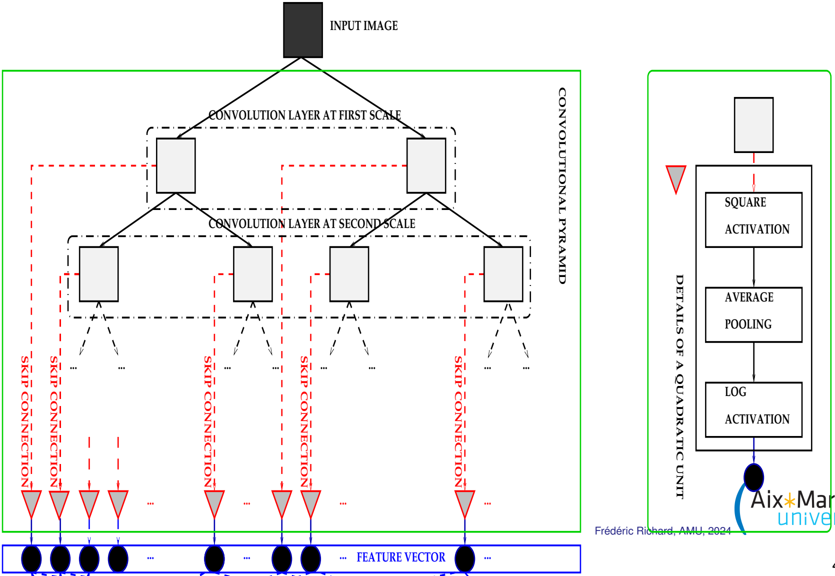

Design of the CNN: complete architecture

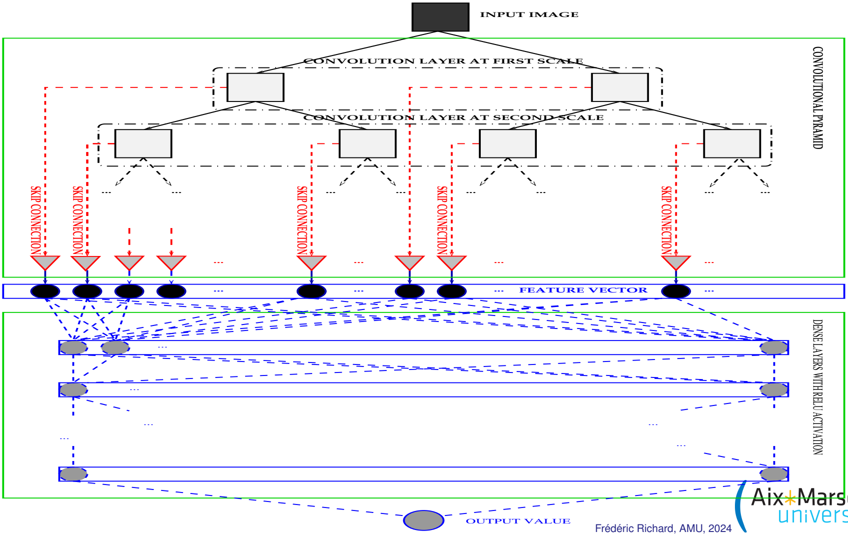

CNN Learning

- Parameter summary:

Layer type	height	size	parameters
Conv pyramid	5	$3 \times 3 + 1$	6 138
Dense layers	8	20 + 1	5 501
Total			11 639

- Generation of a dataset using the package PyAFBF:
  - Images of size 64×64 sampled from AFBF.
  - Parameters of AFBF models are set randomly; the Hurst index is uniformly sampled.
- Set sizes

	Size
Training set	98 000
Validation set	1 000
Test set	1 000
Total	100 000

- Tensorflow (Keras): optimizer (Adam), loss (MSE), batch size (20) , nb epochs (20), time (46 min).

Error analysis

Test error: **1.23 %** (on 1000 images of size 64 $\times$ 64).
to be compared with 3.5 % for the classical method.
Criterium: root mean square error (RMSE, in percent).

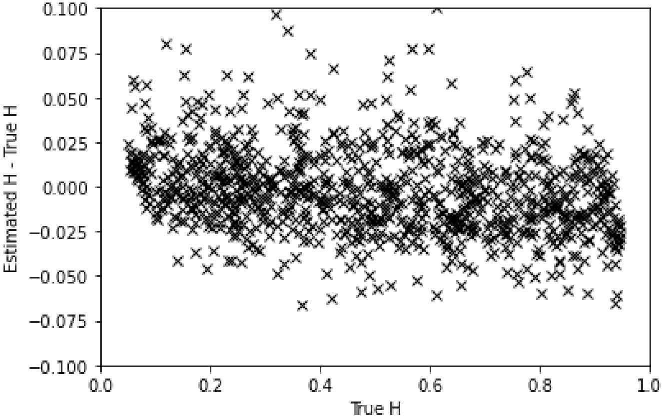

Error as a function of the image size.

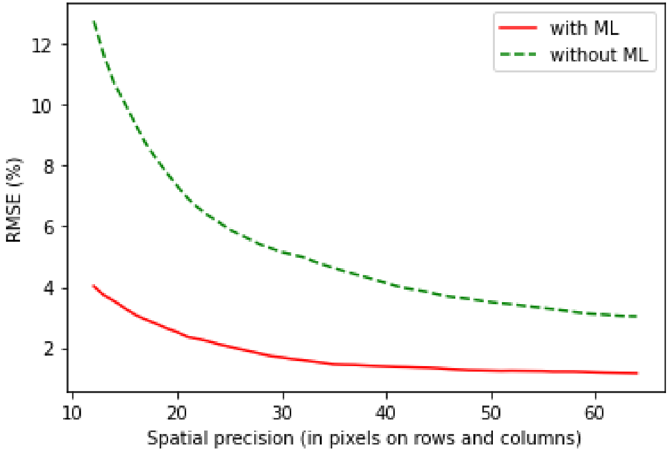

Rmk: a gain of 4 % w.r.t. the classical method.

Application to image segmentation

Image

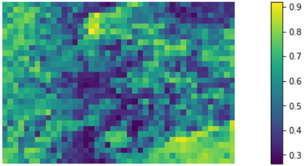

Hurst index estimates

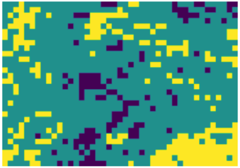

Segmentation

- Source: Max Planck Institute for Meteorology (Understanding Clouds from Satellite Images).
- Processing :
  0.48s per image (1200 $\times$ 1750) with non-overlapping patches (40 $\times$ 40).

Conclusion (Part 2)

- First attempt to use ML for the local estimation of model paramters.
- Good results for the Hurst index.
- Remaining challenges: estimating other parameters.

Benchmark on Kaggle.

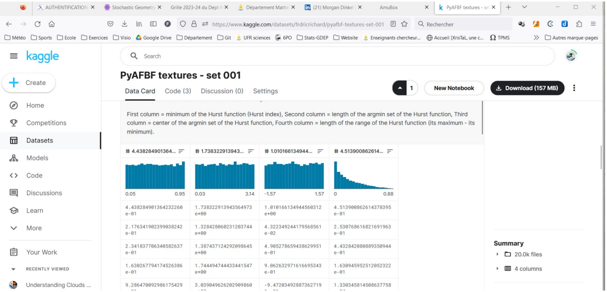

- Repository of 50000 images with associated features.
- Features to estimate from the Hurst function (β):
  - Hurst index: $H = \min_s \beta(s)$.
  - Length of the argmin set: $\mathcal{L}(\arg\min_s \beta(s))$.
  - Center of the argmin set: $\mathcal{C}(\arg\min_s \beta(s))$.
  - Range length: $\mathcal{R} = \max_s \beta(s) - H$
- Features H, $\mathcal{L}$, $\mathcal{C}$ are uniformly distributed over the set.

PyAFBF library.

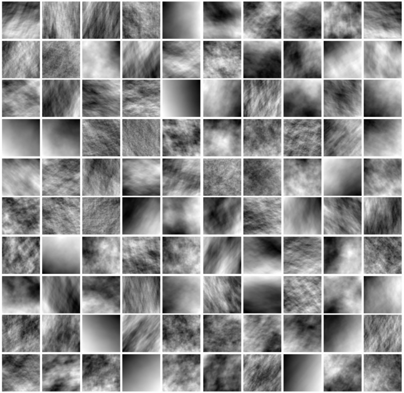

PyAFBF (https://fjprichard.github.io/PyAFBF/), [FR, JOSS, 2022].

- A Python library for sampling image textures from the anisotropic fractional Brownian field.

Estimation of the asymptotic topothesy.

- Z^I: field observed on a grid $\left\{ \left(\frac{i}{I}, \frac{j}{I} \right) \in [\![1, I]\!]^2 \right\}$.
- Increments $V^I_{s,\varphi} = v_{s,\varphi} * Z^I$ at scale s in direction φ.
- Quadratic variations: $W^N_{s,\varphi} = \frac{1}{N_e} \sum_m (V^N_{s,\varphi}[m])^2$.
- Breuer-Major Theorem $\rightarrow$ asymptotic anormality (as I tends to $+\infty$):

$$\log(W^I_{s,\varphi}) = H \ \log(s^2) + \log(\gamma_{H,\tau^*}(\varphi)) + \epsilon^I_u,$$

where

$$\gamma_{H,\tau^*}(\varphi) = \tau^* \circledast \Gamma_H(\varphi) \, \text{with} \, \Gamma_H(\varphi) = \int_{\mathbb{R}^+} |\hat{v}\,(\rho\varphi)|^2 \, \rho^{-2H-1} d\rho.$$

- An inverse problem: Minimize

$$\mathcal{J}(\tau) = \sum_{\varphi} \left(\tilde{\gamma}(\varphi) - \Gamma_{\tilde{H}} \circledast \tau(\varphi) \right)^2 + \lambda |\tau|^2_W.$$

where $\lambda > 0$ and $|\cdot|_W$ is a Sobolev norm.